Al-Nahrain Journal of Science
Al-Nahrain J. Sci., Vol. 29, Issue (3), pp. 91 – 101, September, 2026.

# Assessment of Astronomical Seeing Measurements from KUSZA Observatory (BCK) and Langkawi National Observatory (LNO)

Roslan Umar[1,*], Naqiya Khalidah Hanafiah[2], Nazhatulshima Ahmad[3], Ahmad Hariz Bely[1], Jazeel H. Azeez[4]

[1]East Coast Environmental Research Institute (ESERI), Universiti Sultan Zainal Abidin, Terengganu, Kuala Nerus, 21300, Malaysia
[2]Academy of Islamic Studies, Universiti Malaya, Kuala Lumpur, 50603, Malaysia
[3]Department of Physics, Universiti Malaya, Kuala Lumpur, 50603, Malaysia
[4]Department of Physics, College of Sciences, Al-Nahrain University, Jadriya-10072, Baghdad, Iraq

**Article's Information**

Received: 22.04.2025
Accepted: 21.12.2025
Published: 15.09.2026

**Keywords:**
Astronomical Observation,
Seeing Measurement,
Differential Image Motion Monitor (DIMM),
Full Withd at Half Maximum,
Observatory Site Testing

**Abstract**

This article presents statistical evidence concerning astronomical seeing from the KUSZA Observatory (BCK) and the Langkawi National Observatory (LNO) in Malaysia. Astronomical seeing measurements were performed using a low-cost Differential Image Motion Monitor (DIMM) consisting of an 8-inch Celestron Nexstar and a STV (SBIG) with a CCD camera. A total of four nights of observations were carried out in 2023, namely, 2 nights for each observatory. The median for zenith seeing for the entire observation period at KUSZA observatory was f 2.25" and 2.0" (arcseconds). The results were compared to those obtained previously in February at the LNO. Preliminary results of these measurements indicate that the seeing value in KUSZA Observatory is greater than 2 arcseconds and in Langkawi National Observatory it is about 1 arcsecond. The comparison shows very small differences in the median values between the two measurement sets. The best seeing was observed in BCK on August 26 (median value of 2.0"), while the best seeing observed in LNO was on February 28 (median value 1.3").

http://doi.org/10.22401/ANJS.29.3.09
*Corresponding author: roslan@unisza.edu.my
This work is licensed under a Creative Commons Attribution 4.0 International License

## 1. Introduction

Astronomical seeing refers to the distortion of images of celestial objects caused by optical turbulence in the Earth's atmosphere [1]. Integral seeing includes every individual component of atmospheric turbulence that obstructs the observation. Meteorological science divides the atmosphere into three regions: free atmosphere, boundary layer and ground layer. The wind, temperature and pressure conditions that define the ground layer can affect overall seeing. Since turbulence, which reduces the quality of images directly, monitoring these parameters at the ground reveals the conditions of overall seeing. In astronomy, seeing defines the effective angular resolution attainable, which cannot only be set to a telescope's design mechanism logically, but it is a certainty bound cross interfaced control of the atmosphere. Telescopes are said to have estimated the diameter of power telescopes at λ/D (for D the size aperture and λ the wavelength of light used), yet this estimation is often made unable by atmospheric turbulence. This limit to the angular resolution still remains one of the most problematic factors in ground-based astronomical imaging systems [2]. The cause of the seeing effect arises from high temperature fluctuations resulting from atmospheric turbulence, which scatters incoming starlight due to refractive inhomogeneity [3]. Turbulence modifies the amplitude and phase of electromagnetic waves in transit through the atmosphere [4]. Distortion of the atmosphere gives rise to irregularities in the light wave and when the telescope focuses on these irregularities, it produces a stellar image with

brightness, blurriness and displacement, which is scintillation and blur image motion [5]. These phenomena are produced due to temperature and humidity changes affecting the atmosphere's refractive index. Light passing through inhomogeneously tempered layers undergoes wave distortion that degrades image quality, thus even telescopes are unable to sustain the theoretical angular resolution at the focal length. Refractive turbulence is primarily attributed to winds at lower altitude grounds and temperature differentials between the cooled upper airstream and the heated lower atmosphere. Such turbulence limits the sharpness, precision and ideal conditions needed for ground-based astronomical observations [6].

Although most groundbased telescopes encounter more challenges with the image quality and observational efficiency of the device due to the seeing conditions, the atmosphere remains uncontrolled and long-term tropical atmospheric seeing data are lacking, particularly over Southeast Asia. However, global comprehensive seeing surveys have aided in the site selection and construction planning of principal observatory installations, including Mauna Kea in Hawaii and Maidanak Observatory in Uzbekistan [7]. These locations are advantageous because of their high altitude, dry air and the existence of stable temperature gradients, which make the surroundings permissive for high-quality imaging and adaptive opticals enhanced imaging. On the contrary, equatorial observatories such as those in Malaysia have year round issues with humidity, thermal turbulence and intricate boundary layer phenomena, yet remain grossly absent from international seeing researches. In terms of the telescope in the country, assessing local observatories or evaluating suitable equipment is becoming difficult because empirical data is scarce. Earlier assessments, such as those at Langkawi National Observatory, have certainly enhanced understanding of the phenomenon in Malaysia.

This study works to fill the gap in literature concerning the comparison of atmospheric seeing at Malaysia's two major optical observatories, Langkawi National Observatory (LNO) and KUSZA Observatory (BCK), using the DIMM technique. The study highlights initial standards for stratification of atmospheric turbulence using Full Width of Half Maximum (FWHM) measurements taken on selected nights of 2023. The results will enhance an existing national seeing database while simultaneously guiding observable infrastructure planning, telescope scheduling, equipment configuration and other strategic policies adaptive to Malaysia's environmental conditions.

According to Fried's Theory [8], image degradation caused by atmospheric turbulence is defined by the r_0 parameter, which can be the telescope's diameter that is sufficient for producing a diffraction spot similar in size to that caused by atmospheric turbulence on a point source observed with an infinite mirror. The DIMM evaluates the degree of air turbulence induced aberrations and indicates the seeing FWHM for a big telescope using an ordinary seeing model. The DIMM is a recognized method for evaluating vision. Stock and Keller initially put forward that idea in 1960 [9], while Martin Sarazin, and Roddier investigated its theoretical basis [10]. The DIMM principle measures the positional shifts of a man-made double star created by two telescope sub apertures. When employing the DIMM technique to test the seeing state, the system's optical quality and drive flaws are irrelevant. Measuring a star image's FWHM in a telescope focus is the most common method for assessing the seeing quality. However, such measurements consider both the "image motion" and "image blurring", which are irregular displacements of the image. These techniques frequently encounter motor problems and vibrations of the telescope that cause erroneous image movements. Lower atmospheric turbulence yields relatively low values of seeing, usually represented in arcseconds. At some of the world's best high-altitude observatories like Mauna Kea (Hawaii) at 4,200 meters above sea level average seeing is exceptionally good, as low as 0.4 arcseconds [11].

## 2. Materials and Methods

### 2.1. Site description

The Langkawi National Observatory (LNO) marks one of the most important places in Malaysia for optical astronomical observation. The observatory is located on the island of Langkawi at a height of 111.3 meters above sea level. Its geographic coordinates are 6.34°N latitude and 99.74°E longitude. It is managed by the Malaysia Space Agency (MYSA), which is under the Ministry of Science, Technology and Innovation (MOSTI) [12]. Whereas the KUSZA Observatory is under the management of the Universiti Sultan Zainal Abidin, Terengganu. BCK is located in Merang with 5.54°N and 102.95°E, a seaside location on the East Coast of Peninsular Malaysia and 28 kilometres from Kuala Terengganu city centre, as shown in Figure 1. This observatory lies within a tropical climatic zone, which entails high humidity for the entire year with no distinct cold or dry seasons. In addition, it also serves as a designated site for New Moon sighting activities [13].



(a) (b)

Figure 1: (a) Langkawi National Observatory and (b) KUSZA Observatory

The observations at LNO were conducted in February and those at BCK in August, as these months fall outside the respective monsoon seasons for the west and east coasts are well-documented as periods of lower rainfall, reduced convective activity and more stable atmospheric conditions [13,14], ensuring that both sites were observed during their climatologically optimal windows. The telescope which has the most dominance in both observatory sites is a Celestron NexStar optical telescope, with a 0.203 meter aperture and a 2000 mm focal length. CCD cameras with 1024 × 1024 pixel frames are attached to the telescope, which have 24 × 24 micron sized pixels. Thus, the pixel scale is 1.201 arcseconds, which means it can gauge very fine details and angles of the objects. The resolvable detail of any image depends entirely on the efficiency of the telescope and mounts is fundamental to precise astronomical observations.

### 2.2. Data Collection and Data Analysis

Measuring astronomical seeing is primarily done to mitigate human made turbulence that could interfere with the existing telescopes' performance. Furthermore, image quality verification over time, which is done by accumulating seeing statistics over two nights, aids in the image quality assessment and CCD camera upgrades. Since atmospheric turbulence changes considerably, capturing these needs helps in selecting the correct equipment and precise focusing of the telescope. Therefore, a seeing monitor becomes essential for the operational and planning needs of an observatory. A small reflecting telescope can be employed to construct portable and user-friendly equipment for analysing measurements of astronomical seeing conditions at the sites. A Celestron NextStar 8" reflecting telescope, a CCD camera with STV instruments and a Santa Barbara Instrumentation Group standalone video (SBIG) STV CCD camera, a cardboard mask with two circular holes for implementing the DIMM method (for measuring the seeing values), a laptop computer and a thermometer were used in the research facility to assist the DIMM system. The cardboard mask had two circular openings, each positioned at 80% of the telescope aperture's diameter apart from one another and 20% of the telescope aperture's diameter in size. As for this study, the hole's diameter was 1.6" (4.1cm) and the distance between the centres of the two holes was 6.4" (16.3 cm), as depicted in Figure 2.

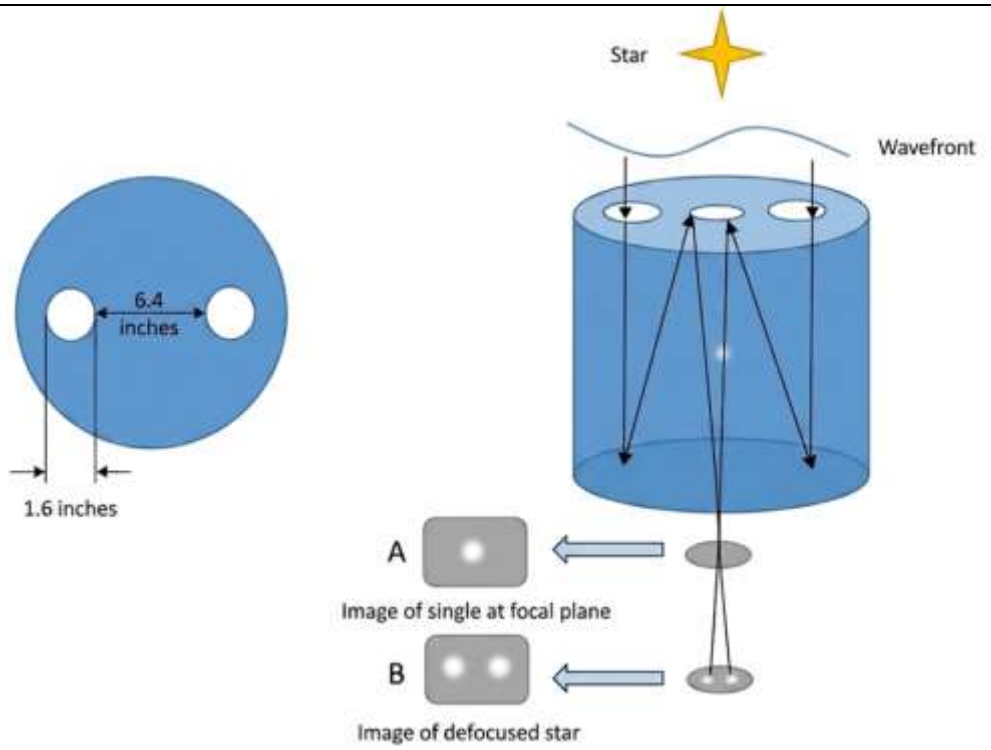



Figure 2: Diagram of the DIMM setup.

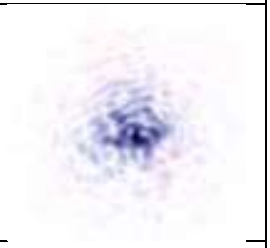
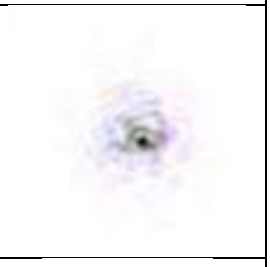
Prior to gauging the measurements, the telescope was pointed at an illuminated star near the zenith (zenith angle ≤30°) and the image was constantly monitored with the STV CCD camera. A mask was then placed over the telescope's front aperture and the focus was slightly adjusted until two distinct spots (representing two closed stars) were clearly visible. Excessive defocusing of the telescope would result in extremely dim images, thus making it difficult for the STV system to differentiate between the two points. Both of these spots should be aligned horizontally on the CCD screen by rotating the mask when necessary. Following that, the STV was set to the seeing monitor mode. In this mode, the STV would find the stars on its own, fine tune the exposure settings and begin data collection. The primary metric used in quantifying astronomical seeing for this study is Full Width at Half Maximum (FWHM). The FWHM defines the angle in arcseconds (″) at which the star's PSF broadens to half its peak value. It corresponds to the degree of atmospheric turbulence FWHM, which indicates the quality of the image. FWHM is measured in arcseconds - the larger the FWHM, the poorer the image [8]. The SBIG STV system worked in seeing monitor mode, which means it would autonomously fetch a bright star and take 32 short exposure snapshots. The STV software computed the two images (with each image generated by the DIMM mask) and calculated the Root Mean Square (RMS) motion of the images, which was then transformed into a seeing figure in arcseconds. To compute the collective metrics for each observing night, the following statistical equations were applied:

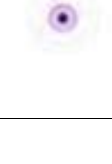
$$Mean = \frac{1}{n}\sum_{i=1}^{n} x_i \quad \ldots(1)$$

where $x_i$ represents each FWHM measurement and n is the total number of valid observations, meanwhile median can be classified as the middle value of the ordered set. So the seeing value of a long exposure stellar image (>5 to 10 seconds) was recorded as the FWHM in arcseconds. As this calculation was based on the RMS relative motion of 32 pictures, the result was not available immediately after entering the mode. While long-term, seasonally distributed observations would indeed strengthen statistical robustness, that will clarify the present results as a preliminary baseline for Malaysia's seeing conditions. Short two night observations are well recognised in the past study as valid for early phase site testing, feasibility studies and instrument validation, as demonstrated by Fuensalida et al. and Mancini et al. [15,16]. Precise measurements will improve with time as more statistical data are

collected. Table 1 provides an example of the Pickering Scale display. To achieve an ideological classification of image sharpness, the Pickering Seeing Scale was employed [17]. This point scale was originally developed by W.H. Pickering, currently used in this work alongside the numerical analysis assessing the Pickering Class of quality of image sharpness or 'seeing' on a scale of 1 to 10. 1 is equivalent to very poor seeing and 10 is excellent seeing. In this work, each FWHM measurement was mapped into a Pickering class along with an interpretation table shown in Table 1. The telescope operator would appreciate the Pickering scale's practical applicability that connects the measurable values of seeing with the experiences visualized while looking through the telescope eyepiece or camera. It is important to note, that at the upper of the scale (Pickering 7–10), the static appearance of stellar images can look very similar when illustrated in diagrams or still photographs. This is because, under good to excellent seeing, the star's point spread function approaches the near diffraction limited Airy pattern, producing a compact central maximum with concentric rings that exhibit only minimal distortion. As a result, the differences between Pickering 7, 8, 9 and 10 are not easily distinguished in static images. In practice, the true distinction becomes evident only when the star is observed in real-time video sequences. Pickering 7 still shows noticeable wobbling of the Airy disk, Pickering 8 exhibits reduced ring motion, Pickering 9 appears almost stable with only slight residual movement and Pickering 10 displays an Airy pattern that is virtually motionless. This dynamic behaviour rather than static morphology is what fundamentally separates the upper high end Pickering classes.

Table 1: Description of image for Pickering scale

| SCALE | D/ $R_o$ | DESCRIPTION | IMAGE |
|---|---|---|---|
| 1 | >5 | The diameter of the star is roughly equal to twice the size of the third diffraction ring, which is approximately 13 arc seconds (13") across. |  |
| 2 | 4 – 5 | The star image is twice the size of the third ring. |  |
| 3 | 3 – 4 | The star image is approximately the same size as the third ring, measuring about 6.7 inches (6.7"), and it's brighter at the center. |  |
| 4 | 2.5 – 3 | The central maxima are often visible; arcs of diffraction rings are sometimes seen on brighter stars. |  |

| | | | |
|---|---|---|---|
| 5 | 2 – 2.5 | Central maxima smeared but always visible; arcs frequently seen on brighter stars. |  |
| 6 | 1.5 – 2 | Central maxima somewhat blurred, always visible; short arcs constantly seen. |  |
| 7 | 1 – 1.5 | Central maxima sometimes sharply defined; diffraction rings seen as long arcs or complete circles. |  |
| 8 | 0.75 – 1 | Central maxima are always sharply defined; rings are seen as long arcs or complete circles, but always in motion. |  |
| 9 | 0.5 – 0.75 | The first diffraction ring remains stationary, while the outer rings are momentarily fixed. |  |
| 10 | <0.5 | The entire diffraction pattern remains stationary. |  |

The numerical representation provided here depends mostly on the fundamental principle of the DIMM method, which generates a correlation between the FWHM and r_0 values. The STV camera incorporates a V-filter in its camera head, while r_0, on the other hand, corresponds to the atmospheric cell size in centimetres, denoting the transverse phase's coherence length, also known as the Fried Parameter. To explain the atmospheric turbulence intensity corresponding to the seeing metrics, this study employs the Fried parameter (r_0), which denotes the coherence diameter of the wave arriving at the telescope. It signifies the largest aperture where the atmospheric phase shifts distortion within one wave, while on the other hand, the theory a lower r_0 means stronger turbulence. With respect to the DIMM method, the stellar image motion of the centroid is defined as the image centroid motion of a star. The RMS motion of the stellar image centroid is used to estimate r_0 through the formula:

$$r_0 = \left\{ \frac{rms^2}{2 \cdot \lambda^2 \cdot (0.179 \cdot d^{-1/3} - 0.0968 \cdot r^{-1/3})} \right\}^{-3/5} \quad \ldots (2)$$

Where $r_0$ is the Fried parameter in meters, rms is the variance of the image separation in radians, λ is the observing wavelength (usually set at 550 nm or $5.5 \times 10^{-7}$m for visual band observations), $d$ is the diameter of each sub-aperture and $r$ is the distance between the centers of the two apertures. This formula captures both the instrumental geometry of the DIMM as well as the wavefront geometry of the incoming wavefront, thus enabling the calculation of turbulence intensity from image motion data. After acquiring $r_0$, the sighting value in arcseconds can be approximated using a simplified expression:

$$FWHM \approx 0.98 \cdot \frac{\lambda}{r_0} \quad \ldots (3)$$

The indicated equation exemplifies seeing quality and Fried parameter having an inverse relationship larger value of $r_0$ means weaker turbulence with improved angular resolution. These formulations collectively explain the interpretation of FWHM values captured by the SBIG STV system during observations at LNO and KUSZA observatories.

## 3. Results and Discussion

This section summarizes analysis results obtained from the LNO and BCK observatories. It crosses examines the data, which evaluates effects attributable to meteorological conditions and discusses aspects of seeing in relation to the visibility and imaging of crescent moons as well as prospects of astronomical endeavors in Malaysia.

### 3.1. Seeing on the site as a comparison.

Using the SBIG STV system, the seeing performance was analyzed for each site over two nights using the DIMM technique. Alongside the data point collection, a total of 32 frames of average stellar image motion were collected per night. Table 2 illustrates the median and mean FWHM values along with Langkawi National Observatory and KUSZA Observatory FWHM performance in Merang, Terengganu. With Langkawi demonstrating a better performance on atmospheric stability terms on February 24 and February 28, with the median seeing values of 1.6” and 1.3”, respectively.

Table 2: Seeing at Selected Observatories.

| Observatory | Date | Max | Min | Mean | Med. |
|---|---|---|---|---|---|
| Langkawi National, Langkawi, Kedah | 24 Feb 2023 | 3.4 | 0.9 | 1.86 | 1.60 |
| | 28 Feb 2023 | 2.8 | 0.6 | 1.56 | 1.30 |
| KUSZA, Merang, Terengganu | 24 Aug 2023 | 3.2 | 0.4 | 1.93 | 2.25 |
| | 26 Aug 2023 | 3.0 | 1.4 | 2.10 | 2.00 |

Accompanied by these figures, the Pickering 6 class levels were reached, which corresponds to moderate seeing conditions rather than good or very high levels of astronomical imaging. In this study, the standard classification where Pickering 1–4 indicates poor seeing, Pickering 5–6 represents moderate seeing, and only Pickering 7–10 reflects good to excellent seeing. For clarity, high resolution imaging typically requires Pickering classes 9–10, where the atmospheric stability is substantially higher than that captured within the preliminary two night dataset. The range of fluctuation was low between 0.9” and 2.5”, representing moderate upper atmosphere stability, which can be explained by the island's isolation, lack of developed surroundings and clean marine airflow. In contrast, the BCK site showed a much higher median seeing of August 24 (2.25”) and August 26 (2.0”) while also demonstrating more turbulent conditions and showing that the Pickering 5 class levels were reached. Though keeping the 0.4” seeing measurement lower than the average represents moments of superior meteorological clarity. Alongside stronger sensitivity to local atmospheric changes of coastal winds and transition season ground layer heating and humidity, seeing fluctuation at BCK has a wider scope, 0.4” - 3.2”. This comparison sheds light on the contrasting site behaviors, which are Langkawi favors steady seeing of good quality while BCK provides intermittent low seeing, which could be appropriate for time-sensitive or automated observation.

### 3.2. Seeing Variability and Optical-Instrument Limitations

Temporal changes with seeing variable atmospheric blurring are, of course, subject to the dynamics of the observing system as well. BCK has a wider range of values, especially on August 24. This is probably due to local meteorological effects such as wind shear and inland thermal mixing. In contrast, Langkawi probably had more stable and thermally quiet marine layers. Other factors are undoubtedly at play. The DIMM method is sensitive to calibration issues among other things. Misalignment of masks and sub-aperture spacing, along with issues of focus and tracking, can affect FWHM. Since the observations were made using a portable system that required extensive hands-on control, it is likely that the average wind value was increased due to poor alignment of the optics. Regardless, the site-specific patterns that were observed and the agreement of the medians indicate that the data reflects the atmospheric seeing, so minor errors of equipment are likely to be insignificant and unorganized.

### 3.3. Seeing Correlation with Light Pollution and Radio Astronomy

The unique features of each site affect how the geographical see. Langkawi's placement of being an isolated island may help explain the lower ranges and medians of seeing values. While no formal light pollution measurements were taken, Langkawi has no main cities, less roads and a few industries. This would make Langkawi an ideal location for long term optics and work on telescopes. Even though BCK is not an urban location, it is in a coastal and not far away from terrestrial interface zone. This may explain the more frequent seeing spikes due to boundary layer turbulence caused by vehicular lights and humid air [18]. For the updated analysis, BCK SQM and L-band RFI values were added to help with situational awareness. In this case, BCK had an SQM of 21.34 mag/arcsec² and an L-band RFI of -82 dBm. LNO also had an SQM of 21.14 mag/arcsec² with an RFI of -81 dBm. This indicates that both locations were comparable in term of sky darkness with good radio quietness. For context, BCK had a representative nighttime surface temperature of 27-28 °C in August, and LNO had a representative nighttime surface temperature of 25-26 °C in February. This represents the differences in monsoon conditions along the east and west coasts [19]. The results from additional seeing research would be more comprehensive if included surface temperature logs and Sky Quality Meters. Environmental and instrumental factors can be better correlated by using these tools. It is worth mentioning, light pollution can indirectly affect seeing in several ways. For example, it can worsen the image motion and degrade the FWHM, since it can enhance the boundary layer turbulence by local heating, increased aerosol scattering and the modification of the nocturnal temperature profile. Radio frequency interference (RFI), which has nothing to do with optical scintillation, can also be a good measure of activity near observatories. Elevated levels of RFI usually mean there is nearby human activity, and thermal plumes that can help to increase the effects of small scale turbulence on optical seeing [20]. Adding RFI and SQM measurements to the studies will improve the environmental dimension of the seeing behavior for the purpose of planning multi wavelength observatories. Multi wavelength applications, applicable at both study sites, expect an increase in demand. Since the sites can potentially host both an optical and radio astronomy facility, the demand for seeing measurements, enhanced with RFI, and SQM studies will also increase [21].

### 3.4. The Role of Seeing in New Crescent Moon Observation and Imaging

New Crescent Moon observations on the other hand, are constrained by atmospheric conditions. During these observations, it is imperative that one captures the faint new crescent as it emerges after the day's setting of the sun. Langkawi's sub 1.5" median values imply that it could provide visual sharpness, especially during New Crescent Moon sightings. Langkawi's low lying marine horizon also means that there is less thermal distortion and visibility is enhanced, this will be continues to support Malaysia's crescent moon observations, especially due to the reasons mentioned before [22, 23]. BCK's value is somewhat more variable, but its best seeing of 0.4″ on August 24 illustrates excellent performance. This indicates that the site can function as a regional Hilal observation station, especially during dry periods, but it also serves as a valuable backup. Additionally, BCK can be used for new crescent moon and planetary imaging, which may be executed with real-time or timely automated capturing during low-seeing periods. Moreover, an increase in seeing directly translates better the quality of the astronomical image's resolution, sharpness of stars' profiles, and increases the accuracy of photometric for astrometric measurements. Results from the assessments strengthen both locations' claims for use in educational astrophotography and other research-

level imaging campaigns with the additional aids of observing sky brightness and moon phase, as well as enabling multi-condition integration. This insightful was shared to the researcher by a passionate amateur astronomy observer and it has been in researcher mind ever since. In our discussion, Malaysians astronomically are fortunate lucky. This has to be the geography factor that Malaysia is positioned almost on the equator, which means most objects from the solar system pass around the zenith where, due to thinner atmosphere, distortion and better seeing conditions. Objects at lower latitude are obstructed by better atmospheric compared to higher geographical latitudes observer. Moreover, relatively weak and less persistent jet stream activity over equatorial latitudes has been widely documented [24, 25], resulting in reduced high altitude turbulence compared to mid latitude regions such as North America. This provides an explanation for the stable planetary imaging conditions that are frequently noted in Malaysia. The absence of strong upper level shear improves the coherence of the wavefront, a necessary prerequisite for sharp high resolution imaging. In addition, relatively weak jet stream activity over Malaysia is another contributing factor to stable atmospheric turbulence. The lack of stable turbulence is a key factor in sharp planetary images. It is the opposite for observers in positioned countries such as the USA. They deal with lower altitude objects and harsh high altitude jet streams that disturb image quality, requiring devices like Atmospheric Dispersion Correctors (ADC). To clarify this further, atmospheric dispersion increases rapidly with zenith distance, producing chromatic elongation of star images; ADCs are therefore commonly required at mid-latitude sites to counter this effect [26]. The equatorial geometry of Malaysian observations where planets often reach higher elevations reduces the magnitude of atmospheric dispersion and consequently lowers dependence on ADC correction. An example of these ADC reliant low image quality targets can be found in an amateur astronomy community compiling storm activity data on Jupiter. In our discussions, if the remaining Malaysian amateur astronomers would actively gather and contribute planetary imagery data, especially regarding Jupiter images, those would become incredibly useful to the astronomy globally. This is due to Malaysia's geographical and atmospheric qualities is good to the astronomical observations. In the revised context, Jupiter is highlighted only as a representative planetary imaging case, illustrating how moments of stable equatorial seeing benefit high resolution observations. The same periods of calm seeing that enable fine Jupiter or Saturn detail also enhance deep space object (DSO) high resolution work, such as double-star separation, compact nebulae structure and fine galactic features.This makes Malaysia appealing to both amateur and professional astronomers. Amateur astronomers can help advance planetary science from Malaysia. This research is the first step to assess the potential of a portable DIMM system when used in real observing contexts in Malaysia. Due to limitations with the available equipment and the weather difficulties, only two nights of observing were possible from each location. While this constrained the scope of the study, it was sufficient to evaluate the system and its methodology. The data collected during the study has the potential to improve the strategies for planning the upgrading of the telescope, the New Crescent Moon observations and support the proposal for creation of the Malaysian Seeing Database. The results also address the gap in observing benchmarks for Malaysia and help frame the establishment of policies on national astronomy along with the Dark Sky sustainability frameworks.

## 4. Conclusions

This preliminary study has shown that a portable DIMM system is able to measure astronomical seeing at Langkawi National Observatory and KUSZA Observatory. Significant data were obtained. Langkawi recorded median seeing values of 1.6″ and 1.3″ Pickering scale 6, while BCK values were 2.25″ and 2.0" Pickering scale 5. The data collected are the first FWHM based benchmarks for Malaysian observatories. The data can be explained based on the site environments, where the effects of local light pollution and near-surface atmospheric disturbance can contribute to the difference in seeing performance at both the sites. Such a relationship shows that the combination of thermal stability and low light pollution results in better seeing, and the importance of such a site evaluation and associated astronomy equipment should be further investigated. The results demonstrate that the long-term monitoring of seeing is feasible and promotes the creation of a Malaysian Seeing Database for assisting the planning of telescopes and the formulation of guidelines on dark skies.

**Acknowledgments:** Special thanks are dedicated to the Electromagnetic Research Group (EMRG) Special thanks are extended to the Electromagnetic Research Group (EMRG) and the Malaysian Space Agency (MySA), particularly Mr. Mohammad Redzuan Tahar and Ms. Farahana Kamarudin, for

their support in providing equipment, facilities and technical assistance throughout this work.

**Conflicts of Interest:** The authors declare no conflict of interest pertaining this work.

**Funding Statement:** This study was supported by the Majlis Agama Islam Dan Adat Melayu Terengganu through the Industry Grant RM015 / UniSZA / 2023 / PPL / MAIDAM (074).

## References

[1] Ahmad, N.; Loon, C. W.; Syukor, M. S.; Haron, S.; Zainuddin, M. Z.; Tahar, M. R.; "The astronomical seeing measurements at Langkawi National Observatory." Int. Conf. Space Sci. Commun. (IconSpace), 2015.

[2] Boumis, P.; Steiakaki, A.; Mavromatakis, F.; Paterakis, G.; Papamastorakis, J.; "Seeing measurements at Skinakas Observatory using the DIMM method." arXiv (Cornell Univ.), 2001.

[3] Cherubini, T.; Businger, S.; Lyman, R.; Chun, M.; "Modeling Optical Turbulence and Seeing over Mauna Kea." J. Appl. Meteor. Climat. 47(4): 1140–1155, 2008.

[4] Darudi, A.; Nasiri, S.; "Designing and making a differential astronomical seeing monitor." Iranian J. Phys. Res. 5(3): 121–128, 2019.

[5] Ismail, K.; Asillam, F.; Zin, A. A. M.; "Human resource development issues in the field of Islamic astronomy: Analysis of the Langkawi National Observatory, Malaysia." Int. J. Soc. Sci. Humanity 4(6): 463–467, 2014.

[6] Ma, B.; Shang, Z.; Hu, Y.; Hu, K.; Wang, Y.; Xu, Y.; Ashley, M. C. B.; Hickson, P.; Jiang, P.; "Night-time measurements of astronomical seeing at Dome A in Antarctica." Nature 583(7818): 771–774, 2020.

[7] Tokunaga, A. T.; "New generation Ground-Based Optical/Infrared telescopes." Encycl. Sol. Syst.: 1089–1105, Elsevier, 2014.

[8] Fried, D. L.; "Optical resolution through a randomly inhomogeneous medium for very long and very short exposures." J. Opt. Soc. Am. 56(10): 1372–1379, 1966.

[9] Munõz-Tuñón, C.; Vernin, J.; Varela, A. M.; "Night-time image quality at Roque de los Muchachos Observatory." Astron. Astrophys. Suppl. Ser. 125(1): 183–193, 1997.

[10] Sarazin, M.; Roddier, F.; "The ESO differential image motion monitor." Astron. Astrophys. 227: 294–300, 1990.

[11] Tillayev, Y.; Azimov, A.; Ehgamberdiev, S. A.; Ilyasov, S.; "Astronomical seeing and meteorological parameters at Maidanak Observatory." Atmosphere 14(2): 199, 2023.

[12] Bely, A. H.; Umar, R.; Sabri, N. H.; Abidin, Z. Z.; Nasir, A. L. A. M.; Ismail, I.; ...; Rakhmadi, A. J.; "Light Pollution Monitoring Through Zenithal Sky Brightness at Selected Malaysian Observatories." J. Phys.: Conf. Ser. 2915(1): 012003, 2024.

[13] Loh, J. L.; Tangang, F.; Juneng, L.; Hein, D.; Lee, D. I.; "Projected rainfall and temperature changes over Malaysia at the end of the 21st century based on PRECIS modelling system." Asia-Pac. J. Atmos. Sci. 52(2): 191–208, 2016.

[14] Lolli, S.; Khor, W. Y.; Matjafri, M. Z.; Lim, H. S.; "Monsoon season quantitative assessment of biomass burning clear-sky aerosol radiative effect at surface by ground-based lidar observations in Pulau Pinang, Malaysia in 2014." Remote Sens. 11(22): 2660, 2019.

[15] Fuensalida, J. J.; García-Lorenzo, B.; Hoegemann, C.; "Correction of the dome seeing contribution from generalized-SCIDAR data using evenness properties with Fourier analysis." Mon. Not. R. Astron. Soc. 389(2): 731–740, 2008.

[16] Mancini, D.; Auricchio, A.; Brescia, M.; Ortolani, S.; Porceddu, I.; Sansone, M. P.; Zitelli, V.; "The Galileo Telescope seeing monitor: Technical overview and first results." New Astron. Rev. 42(6–8): 425–429, 1998.

[17] Mat, R.; Hazmin, S. N.; Umar, R.; Ahmad, S.; Zafar, S. N. A. S.; Marhamah, M. S.; "The modelling of tropical weather effects on Ultra-High Frequency (UHF) radio signals using SmartPLS." IOP Conf. Ser.: Mater. Sci. Eng. 440: 012041, 2018.

[18] Pickering, W. H.; "The Moon: A Summary of the Existing Knowledge of Our Satellite, with a Complete Photographic Atlas." New York: Doubleday, Page & Co., 1909.

[19] Umar, R.; Azan, M. A. I. A.; Sabri, N. H.; Ngah, N.; Zulkeflee, A. N.; Mohamad, A. E.; ...; Nasir, A. L. A. M.; "Model Reruang Magnitud Kecerahan Langit Di Balai Cerap KUSZA, Universiti Sultan Zainal Abidin (UNISZA)." Sains Malaysiana 52(10): 2943–2954, 2023.

[20] Hassan, F. N.; "OPTIMAL PROJECTION FROM N-DIMENSIONAL PATTERNSPACE INTO A PLANE." Al-Nahrain J. Sci. 12(1): 149–155, 2009.

[21] Bely, A. H.; Nasir, A. L. A. M.; Umar, R.; Chik, W. M. Y. W.; Husaini, R.; Othman, M. S.; Rakhmadi, A. J.; "Empowering Astronomical Exploration: Advancement of New Moon Observation Devices in Sarawak, Malaysia." Iraqi J. Sci.: 6154–6162, 2024.

[22] Teixeira, M. A. C.; Argain, J. L.; "The dependence of mountain wave reflection on the abruptness of atmospheric profile variations." Q. J. R. Meteorol. Soc. 146(729): 1685–1701, 2020.

[23] Olson, J.; Prather, M.; Berntsen, T.; Carmichael, G.; Chatfield, R.; Connell, P.; ...; Wild, O.; "Results from the Intergovernmental Panel on Climatic Change photochemical model intercomparison (PHOTOCOMP)." J. Geophys. Res.: Atmos. 102(D5): 5979–5991, 1997.

[24] Filippenko, A. V.; "The importance of atmospheric differential refraction in spectrophotometry." Publ. Astron. Soc. Pac. 94(560): 715, 1982.

[25] Pathak, P.; Guyon, O.; Jovanovic, N.; Lozi, J.; Martinache, F.; Minowa, Y.; ...; Narita, N.; "A high-precision technique to correct for residual atmospheric dispersion in high-contrast imaging systems." Publ. Astron. Soc. Pac. 128(970): 124404, 2016.

[26] Bely, A. H.; et al.; "The limitation of optical equipment in new crescent moon visibility: Insight from 27 years of observation data in Sarawak, Malaysia." Sains Malaysiana 54(9): 2263–2276, 2025. https://doi.org/10.17576/jsm-2025-5409-13